Superalloys 718, 625, 706 and Various Derivatives
Edited by E.A. Loria
TMS (The Minerals, Metals & Materials Society), 2001

Effect of Cooling Rate on Microstructural Development in Alloy 718

A. D. Patel and Y. V. Murty

Carpenter Technology Corporation
101 W Bern St., Reading, PA 19601

ABSTRACT

A variety of cast Pyromet® 718 alloy microstructures result from processing of different diameters of industrial scale ingots for producing superalloy forgings used in aircraft turbine engine applications. The hot workability of these cast alloys will significantly depend on the cast microstructure. The current study is focussed on understanding the evolution of the cast microstructure during Vacuum Arc Remelting (VAR) of 718 superalloy as it relates to secondary dendrite arm spacing, second phase evolution and distribution during solidification. The variation microstructure is related to different cooling rates encountered in superalloy production. The effect of cast structure on homogenization and hot working is also discussed.

INTRODUCTION

Carpenter Pyromet® 718 alloy, also known under a variety of trade names which is covered by UNS NO7718 designation, is a very important structural material used in Aero and Power generation industries. Oxidation resistance, creep resistance, fatigue resistance, wear resistance, and strength at elevated temperatures of this alloy make it most suitable in both rotating and stationary structural components operated at high temperatures. Therefore, there is significant interest in optimizing processing of this alloy to obtain better homogeneity, and improved process yield. In recent years, the demand for larger structural components in gas-powered land-based turbine engines has also increased. These trends/needs point to producing larger diameter starting ingot stock to be forged into appropriate billet size for further isothermal forging into final parts /1/. This places challenging demands on primary materials producers to develop processing technology to produce larger diameter triple melted ingots and develop appropriate thermo-mechanical treatments to produce the forge billets with highly uniform chemistry and grain size. As a consequence, there is an ever-increasing need to understand the cast microstructure with respect to cast grain size, micro and macro-segregation of alloying elements, homogenization kinetics, and individual or combined effects on hot formability and final microstructure of the billet.

The typical composition of alloy 718 is shown in Table I. This alloy metallurgy is designed to provide exceptionally good mechanical properties at temperatures as high as 700 °C. The role of each alloying element is also shown in Table I /2/. While this alloy chemistry is designed to accomplish very specific functional performance, it is extremely

Table 1: Typical chemical composition and effects of alloying elements in alloy 718

Element	Weight %	Effects
C	0.08 max	Forms carbides.
Cr	17-21	Forms oxide layer for oxidation and corrosion resistance and may form $Cr_{23}C_6$ carbides
Ni	50-55	Base element for austenite matrix. Forms the strengthening phase (γ", and δ), provides high temperature strength
Mo	2.8-3.3	Solid solution strengthening element, and provides corrosion resistance.
Nb	4.75-5.50	Forms primary strengthening phases γ" (Ni_3Nb). Combines with carbon to form NbC carbides.
Ti	0.65-1.15	Forms primary strengthening phases, γ' (Ni_3Ti) and forms TiC carbides.
Al	0.2-0.8	Forms and stabilizes primary strengthening phase (γ")
B	0.006 max	Refining element, which benefits hot ductility
Fe	Balance (~18)	Forms Laves, $Fe_2(Nb,Mo)$

important to precisely control the chemistry during processing. Particularly important is the chemistry during the triple melting practice often required for many applications. The final cast microstructure is established during VAR, which is the third melting operation. Of the alloying elements present in the alloy, niobium is the most difficult to control due to its severe segregation tendency during solidification, the partition ratio is about 0.5. Niobium, therefore is the subject of many investigations.

The physical metallurgy of alloy 718 is well described by Radavich /3/. The structural evolution during hot working of this alloy is further reviewed by Jones et al. /4/. While there is extensive literature published on this alloy, most work was focussed on hot working and final property control. Most solidification related studies are focussed on macro-segregation aspects of solidification, particularly freckles and white spots /5-6/. The understanding of the mechanism of defect formation has resulted in optimization of VAR processing parameters such as power input, electrode quality and cooling during melting. These studies provide the guidelines to producing quality ingots consistently, which, in turn, has increased the reliability and performance of the components made from this alloy.

The purpose of the present investigation is to systematically understand the solidification behavior of alloy 718 under a variety of cooling conditions typical to that of those existing in the industrial processes. The industrial processes used to manufacture the alloy include Vacuum Induction Melting (VIM), Electroslag Remelting (ESR), and Vacuum Arc Remelting (VAR). The cooling rates studied herein cover a full range of ingot diameters normally produced in the industry. The effect of these cooling rates, which determine the cast microstructure and the solidification behavior, was studied with a goal of understanding the final ingot structure and its response to homogenization treatments.

EXPERIMENTAL PROCEDURE

During this investigation, the base line information on cast microstructural features like dendrite arm spacing was obtained from sections taken from different VAR processed alloy 718 ingots, covering a range from laboratory scale (8") to industrial scale (> 20"). The solidification structure depends on cooling rate, which is determined by the processing parameters for each cast ingot. The cooling rates were calculated from the temperature distribution in the ingot. The temperature profile in the ingot was obtained from a mathematical model developed by the Specialty Metals Processing Consortium (SMPC). The model is routinely used to determine the effect of melting parameters like power input, ingot diameter and cooling conditions on the temperature profile and the flow in the solidifying ingot. The details of the model are published elsewhere /7,8/.

The isothermal heat treatment experiments were conducted on small samples (2"x 3/4"x 3/4") cut from the cast ingot. The pieces were heated to a predetermined temperature in the mushy zone in a small resistance furnace. Each sample was held at temperature for 2 hrs in an inert gas blanket and immediately water quenched. The samples were cut along the cross-section, polished and etched using standard metallographic techniques. The volume fraction of liquid was measured by the point counting technique, using a 3 mm grid /9/.

RESULTS

The SMPC model was used to determine the temperature distribution in the ingot. During quasi-steady melting, the cooling rate in the ingot can be determined from the product of the casting rate and the temperature gradient in the mushy region. The casting rate is obtained from the processing parameters for each ingot and the temperature gradient in the mushy zone is obtained from the mathematical model. Thus the secondary dendrite arm spacing (SDAS), is obtained from the following relationship /10/:

$$SDAS = C\left(\frac{T_l - T_e}{\dot{T}}\right)^{1/3} \qquad (1)$$

Where SDAS is in μm , C is a constant and for alloy 718 is about 10; T_l is the liquidius temperature; T_e is the eutectic temperature (γ/laves); and $\dot{T}$ is the cooling rate (°C/sec). The thermo-physical properties and solidification parameters for these calculations were obtained from literature /11-12/.

Figure 1 shows a plot of the calculated and measured SDAS at different cooling rates expressed as a function of the dimensionless ingot radius. As can be seen, the comparison is reasonably good; the model predictions are within the bounds of the experimental measurements. The experimental measurements were made from longitudinally sectioned samples from the cast ingots. Samples were taken from different locations in the ingot. For metallographic analysis, the samples were mounted in Bakelite, polished and etched using a solution of hydrochloric acid and hydrogen peroxide. The resulting microstructure (25X) from the three representative cooling histories are inserted into Figure 1. Each measured SDAS point represents an average value of 30 measurements at each location with one standard deviation of about 10 μm.

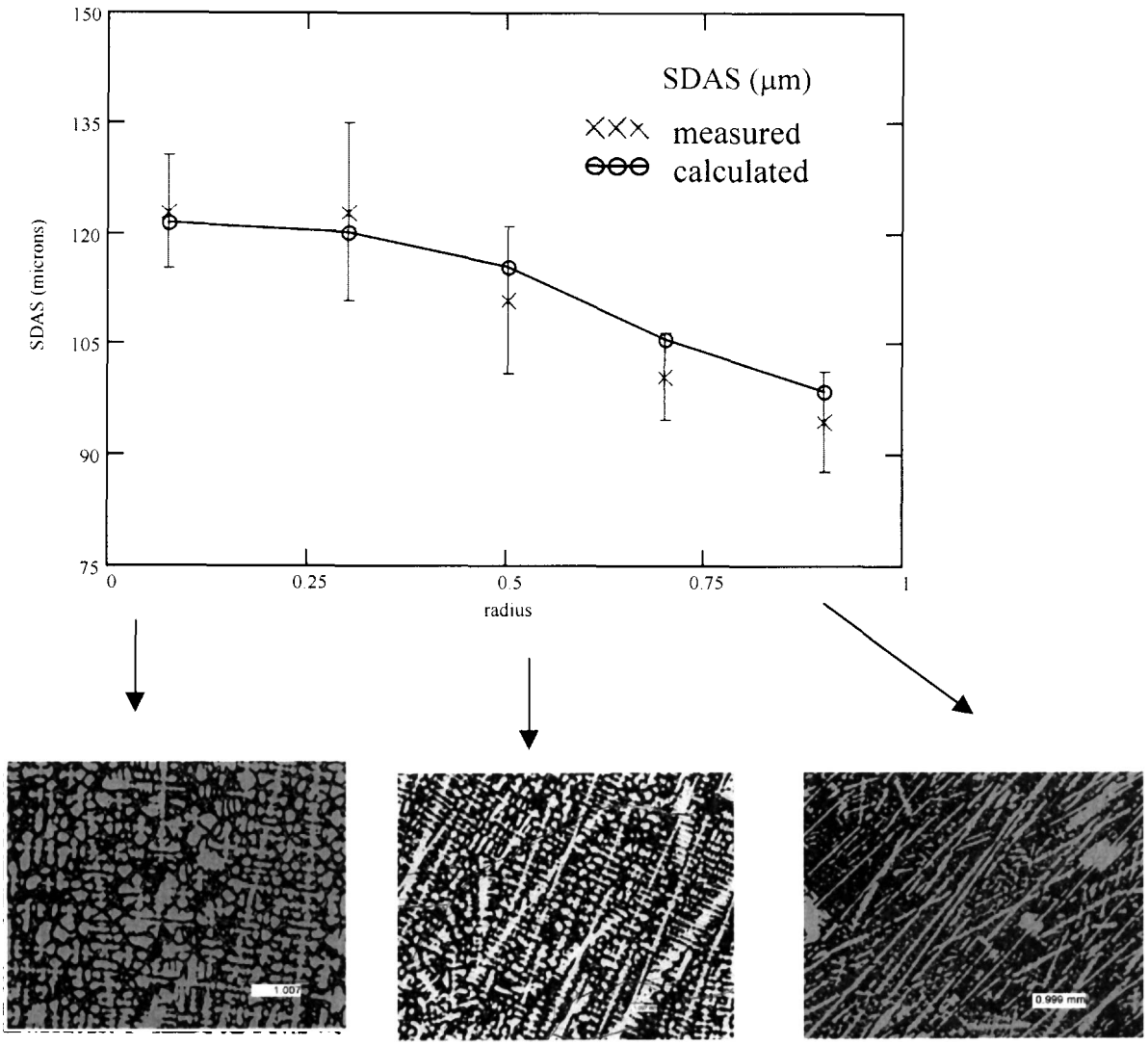

Figure 1: Comparison between measured and calculated SDAS along the radius of an alloy 718 ingot processed under nominal melting parameters. Also shown are the microstructures at 25X at the ingot center, mid-radius and surface. Each sample was immersed for 20-40 sec. in a 90 mL HCl + 10 mL H_2O_2 (3%) solution.

After benchmarking the model, simulations were carried out for a variety of ingot diameters using nominal processing parameters for each case. The overall heat transfer coefficient at the ingot surface was varied between 350 W/m^2 K to 400 W/m^2 K, which covers large and small diameter ingots /13/. As described above, from the temperature distribution in the ingot, the cooling rate was determined at different radial locations. Figure 2 shows the SDAS variation as a function of cooling rate. The cooling rates and corresponding SDAS can vary significantly as a function of the ingot diameter. The SDAS, studied herein, varied between 220-80 μm with a corresponding cooling rate band of 0.01- 0.33 °C/sec. As will be discussed later, the significance of this variation in SDAS relates directly to the homogenization kinetics of the cast ingot and the resulting consequences in further hot-forging operation.

The niobium concentration was measured using a Cameca SX-100 microprobe. Analysis was conducted with an accelerating voltage of 20 kV, probe current of 40 nA, and a

spot size of about 1 μm. A 500-μm^2 area was scanned using a square grid, with measurements taken at every 50-μm with a total of 100 measurements. The fraction of solid was obtained by ordering the data and dividing each data point by the total number of measurements /14/. Figure 3 shows the niobium microsegregation profile for different cooling rates with SDAS ranging from 120-100 μm.

Alloy 718 has a large solidification range. This difference between the liquidus and solidus of the alloy and the cooling history in this mushy zone region establishes the castability of this alloy as well as the quality of the cast ingot. This temperature range, governed by the chemical constitution, establishes the solidification pattern of the alloy. The solidification sequence in this alloy, described in detail by Knorovsky et al., consists of primary γ matrix followed by two eutectic-like reactions /15/. The first eutectic-like reaction results in niobium carbides and the second eutectic-like reaction results in the niobium rich lave phase. As solidification progresses inter-dendritic liquid gets rich in Nb, Ti, Mo and C.

Figure 4 shows the microstructure of a sample heated to 1275 °C followed by water quenching. The small globular restructure is the liquid. Figure 5 shows the volume fraction of solid in the mushy region. The fraction of solid does not decrease linearly with temperature; as the temperature drops from 1325 to 1300 °C, the fraction of solid decreases rather steeply to 0.6. At 1275 °C, the fraction of solid is about 0.8. The measured solid fraction is in good agreement with that calculated using the Scheil equation,

$$f_s = 1 - \left[1 + \frac{1}{C_o}\left(\frac{T - T_l}{m_L}\right)\right]^{1/k-1} \qquad (2)$$

Where, C_o is the bulk composition, k is the partition ratio, the slope of the liquidus in the pseudo binary system, m_L, is obtained using the eutectic composition, C_e, and is given by $m_L = (T_e - T_l)/(C_e - C_o)$.

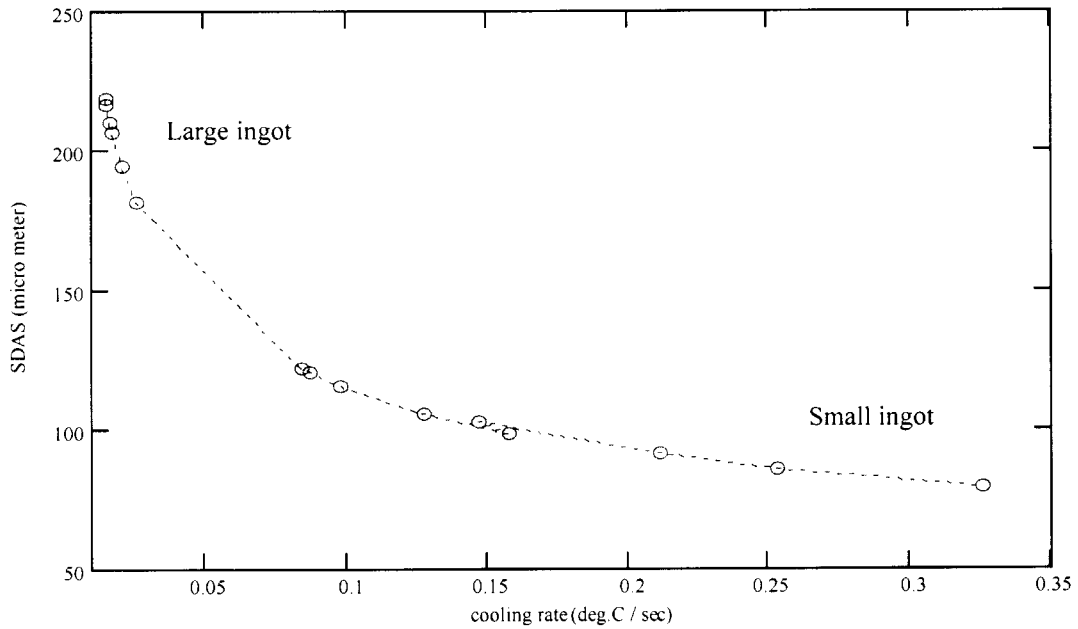

Figure 2: SDAS variation with cooling rate for different diameter VAR processed alloy 718 ingots.

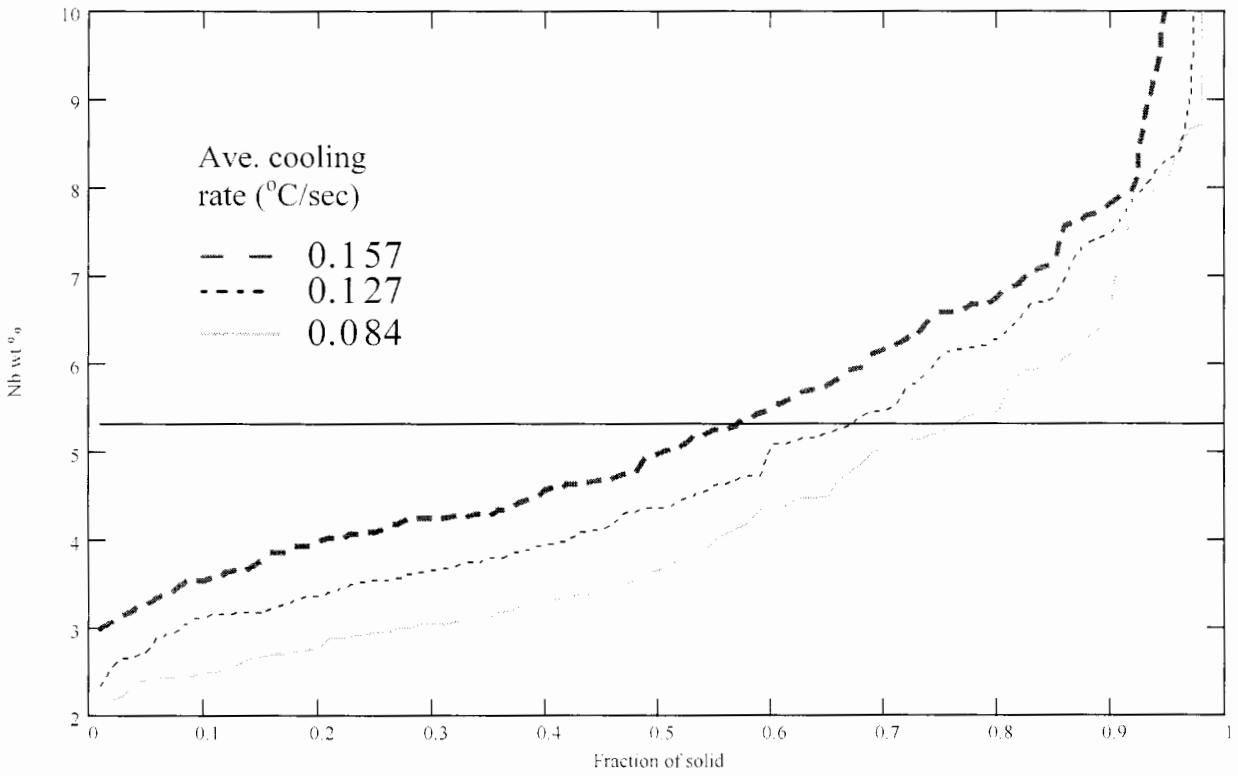

Figure 3: Microsegregation in alloy 718 ingot at different cooling rates. 100 measurements were taken in a 500-μm^2 area. Horizontal line is the bulk composition.

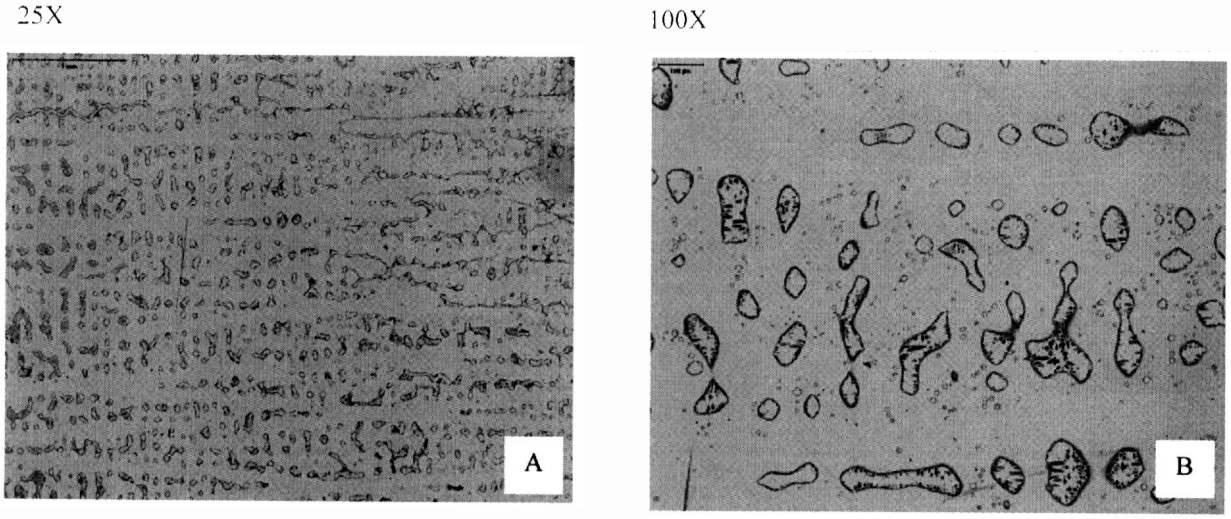

Figure 4: Typical microstructure of alloy 718 after water quenching from 1275 °C, the small globules represent the liquid (A) at 25 X, (B) at 100X.

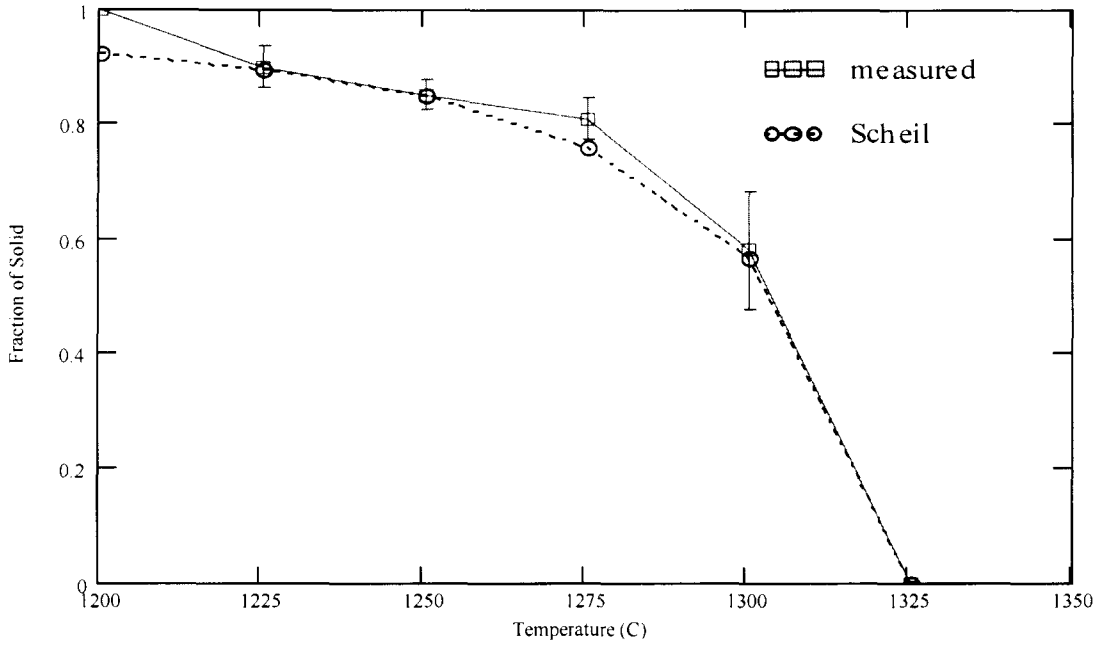

Figure 5: Volume fraction of solid as function of temperature in the mush region for alloy 718. The bulk composition, C_o=5.3 wt % Nb, and m_l = -9.1 °C/wt pct. The partition ratio measured by a line scan across the liquid-solid region on the microprobe was 0.496.

DISCUSSION

As the cooling rate decreases, the SDAS increases; in industrial size VAR ingots, the cooling rate varies from 0.01- 0.33 °C/sec, with a corresponding SDAS value between 220-80 microns. Thus, an order of magnitude difference is typical in current industrial scale ingots. There is more segregation of solute within the dendrite cell at the ingot center than the surface, where the cooling rate can easily be twice that of the center. Figure 6 shows the partition ratio as a function of cooling rate for alloy 718. Nb, Mo, and Ti have k values lower than unity, indicating that these elements segregate in interdendritic liquid. On the other hand, Cr and Fe, with k value greater than unity, segregate in the dendrites. At low cooling rates, the downward flow of the heavier interdendritic fluid results in remelting of the solute lean solid, thereby forming freckles /16/.

During solidification in alloy 718, once the composition of the growing dendritic phase reaches 9.3 wt % Nb, the remaining liquid transforms in to the γ/laves eutectic constituent. Figure 3 shows that at a cooling rate of 0.157 °C/sec, the fraction of eutectic is 0.06, and decreases to 0.03 at 0.127 °C/sec and is 0.02 at 0.084 °C/sec. At lower cooling rates, there is enough time for back diffusion in the solid (solidification time is greater than diffusion time); hence, a lower fraction of the eutectic laves phase. This suggests that in large ingots the volume fraction of laves is the highest at the surface and decreases towards the ingot center.

The partition ratio for niobium in alloy 718 typically varies from about 0.4 at the center to 0.56 at the ingot surface. At the center of a typical VAR ingot, niobium could vary from 2 wt % at the dendrite core to 10 wt % in the interdendritic region. The cast ingots are homogenized at a temperature below the solidus temperature to reduce both interdendritic as well as dendritic coring. Assuming a linear initial concentration, the time scale, τ, for homogenization can be calculated from the analytical solution of the diffusion equation and is given by:

$$\tau = 3\frac{L^2}{\pi^2 D_s} \tag{3}$$

where: L is one half the SDAS and D_s is the diffusion coefficient. It should be noted that the time scale is proportional to the square of the secondary dendrite arm spacing. The effectiveness of a homogenization treatment is expressed in terms of a residual segregation index, δ /17/. In the as cast condition, δ is unity, and after homogenization, δ approaches 0. Figure 7 shows a plot of the segregation index for different SDAS. As seen, the homogenization time for a SDAS of 100 μm is about 26 hrs at temperature.

Reduction in alloy segregation through homogenization is critical to the hot formability of the material in subsequent forging operations. The higher the homogeneity of the cast material, the lower the deformation force required to achieve certain strain in the billet and associated penetration from the surface to the center of the billet. The homogeneity is further improved as the material gets forged to lower billet diameter followed by the intermediate reheat required to maintain the forging temperature range to achieve uniform deformation and reduce cracking. Therefore, prior knowledge of cast microstructure is essential for proper design of thermomechanical treatments necessary to achieve consistent grain size through the entire cross section of the forge billet. The higher the dendrite arm spacing, the longer the homogenization time required to reduce the elemental segregation. Thus, as the ingot diameter gets larger, it is important to retune the thermomechanical processing to the new cast microstructure.

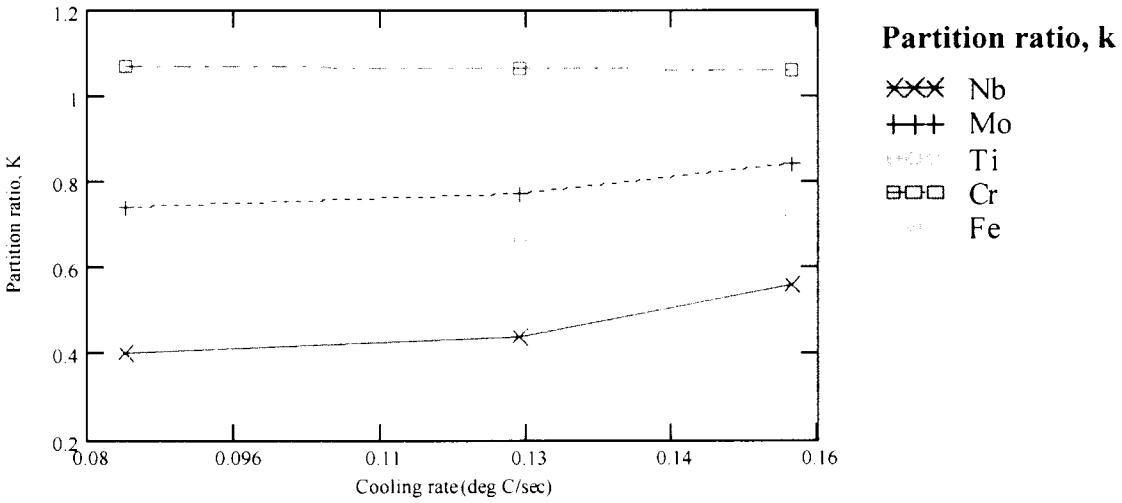

Figure 6: Partition ratio, $k = \frac{C_{min}}{C_{bulk}}$, as function of cooling rate in alloy 718.

CONCLUSION

The cooling rate in industrial scale Vaccum Arc Remelted alloy 718 ingots studied herein varied in the range of 0.01- 0.33 °C/sec with a corresponding SDAS between 220-80 μm. In the as-cast VAR ingots, the niobium concentration could vary from 2 wt % at the dendrite core to 10 wt % in the inter-dendritic region. Depending on the local cooling rate the partition

ratio ranges between 0.4-0.56. The volume fraction of eutectic constituent is higher at the ingot surface than the center. The time scale for homogenization of the cast ingots is proportional to the square of the dendrite arm spacing. After homogenization, the residual segregation index is typically about 0.05. Reduction in segregation is critical for subsequent forging operations, especially in large diameter ingots.

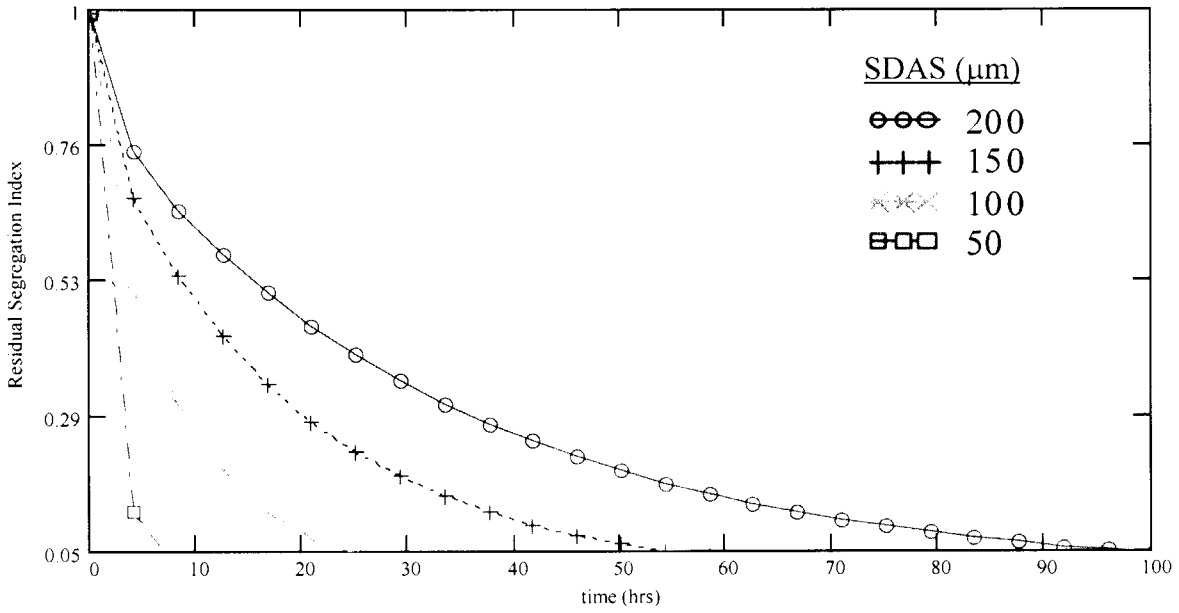

Figure 7: Variation of the Residual Segregation index with homogenization time for different secondary dendrite arm spacing. The diffusion coefficient at the homogenization temperature of 1177° C is about 8 10^{-15} m^2/sec /18/.

ACKNOWLEDGEMENT

The authors would like to acknowledge the help of Keith Hill for all the microprobe analysis, Gregory Miller, Frederick Miller and Jesse Lesher for assistance in metallography.

REFERENCES

1. R. C. Schwant et al., "Large 718 Forgings for Land Based Turbines," Superalloys 718, 626, 706 and Derivatives, ed. E. A. Loria (TMS, 1997) 141-152.
2. Ronald C. Gebeau, private communication with author, Carpenter Specialty Alloys, 6 March 2001.
3. J. F. Radavich, "The Physical Metallurgy of Cast and Wrought Alloy 718," Superalloy 718, E. A. Loria (TMS, 1989) 229-240.
4. R. M. F. Jones and L. A. Jackman, "The Structural Evolution of Superalloy Ingots During Hot Working," Journal of Metals, January (1999), 27-31.
5. L. A. Jackman, G. E. Maurer, and S. Widge, "New Knowledge About White Spots in Superalloys," Advanced Materials and Processes, 5 (1993), 18-25.
6. P. Auburtin et al., "Freckle Formation and Freckle Criterion in Superalloy Castings", Metallurgical and Materials Transactions B, 31 (2000), 801-811.

7. L. A. Bertram et al., "The Macroscale Simulation of Remelting Processes," Journal of Metals, 50 (1998), 18-21.
8. L. A. Bertram et al., "Transient Melt Rate Effects on Solidification During VAR of 20-Inch Alloy 718," Proceedings of the International Symposium on Liquid Metal Processing and Casting, ed. A. Mitchell, L. Ridgway, M. Baldwin (AVS, 1999), 156-167.
9. G. F. Vander Voort, Metallography Principles and Practice, (ASM International, 1999), 426-432.
10. W. Kurz and D. J. Fisher, Fundamentals of Solidification (Switzerland: Trans Tech Publications, 1998), 85.
11. P. N. Quested et al., "Physical Property Measurements for Simulation Modeling of Heat and Fluid Flow During Solidification," Proceedings of the International Symposium on Liquid Metal Processing and Casting, ed. A. Mitchell, P. Auburtin (AVS, 1997), 1-17.
12. L. Nastac and D. M. Stefanescu , "Computational Modeling of NbC/Laves Formation in Inconel 718 Equiaxed Castings," Metallurgical and Materials Transactions , 28A, (1997), 1582-1587.
13. K. O. Yu, "Comparison of ESR-VAR Processes-Part1: Heat Transfer Characteristics," Proceedings of the International Symposium on Liquid Metal Processing and Casting, ed. A. Bhatt (AVS, 1984), 83-92.
14. M. N. Gungor, "A Statistically Significant Experimental Technique for Investigating Microsegregation in Cast Alloys", Metallurgical Transactions, 20A, (1989) 2529-2533.
15. G. A. Knorovsky et al., "Inconel 718: A Solidification Diagram," Metallurgical Transactions, 20A, (1989), 2149-2158.
16. J. A. Van Den Avyle et al., "Reducing Defects in Remelting Processes for High-Performance Alloys," Journal of Metals, 50 (1998), 22-25.
17. M. C. Flemings, Solidification Processing (New York: McGraw-Hill Book Company, 1974), 328.
18. W. J. Boettinger et al., "Development of Multicomponent Solidification Micromodels using a Thermodynamic Phase Diagram Data Base," Modeling of Casting, Welding and Advanced Solidification Processes V11, ed. M. Cross and J. Campbell, (TMS 1995), 649-656.